Mesoscale Rainbands in Extratropical Cyclones[1]

ROBERT A. HOUZE, JR., PETER V. HOBBS, KUMUD R. BISWAS AND WILLIAM M. DAVIS

Department of Atmospheric Sciences, University of Washington, Seattle 98195

(Manuscript received 30 January 1976, in revised form 19 April 1976)

ABSTRACT

Mesoscale rainbands (5–50 km in average width and hundreds of kilometers in length) have been found in eleven extratropical cyclones. Six types of rainbands have been identified (warm frontal, warm sector, cold frontal—wide, cold frontal—narrow, wave-like, post-frontal). Comparison with extratropical cyclone data from various parts of the world indicates that these rainband types occur rather generally in mid-latitude cyclones.

The rainbands examined in this study contained small-scale areas of especially concentrated rainfall. These small-scale elements were 10–500 km² in area, occurred in concentrations of 1–3 per 1000 km², and moved with the wind between 850 and 700 mb.

1. Introduction

It is now generally recognized that the rainfall in extratropical cyclones tends to be concentrated within mesoscale areas, which have horizontal dimensions of tens to hundreds of kilometers (Harrold and Austin, 1974; Browning, 1974). The largest mesoscale areas tend to be elongated, with lengths exceeding widths by a factor of 2 or more. In this paper such elongated features are referred to as rainbands (or bands for short).

Since 1973, the Cloud Physics Group at the University of Washington has been engaged in an intensive study of cyclonic storms in western Washington known as the CYCLES (CYCLonic Extratropical Storms) Project. As part of the CYCLES Project we have undertaken a survey of the mesoscale structure of rainfall in occluded cyclones. In this paper we present examples of the rainbands which were observed in these storms and suggest a classification scheme for them. Previous investigators have elucidated the structure of individual rainbands in case studies and in review papers. Harrold and Austin (1974) and Browning (1974) have generalized these results to some degree. However, their reviews do not include all of the types of rainbands which we have observed in the Pacific Northwest, and we have therefore developed a general classification scheme which combines our observations with previous results in one convenient summary. This morphological classification scheme provides a useful background to our other studies of cyclonic storms which focus on the dynamical and cloud microphysical processes associated with rainbands (Hobbs *et al.*, 1975; Houze *et al.*, 1976).

[1] Contribution No. 373, Department of Atmospheric Sciences, University of Washington.

2. Locations of studies and facilities

Two types of studies were conducted. The first type (referred to as the Pacific Ocean studies) focussed on precipitation patterns occurring over a region of the Pacific Ocean extending west of the Washington State coastline. The primary facility for these studies was a large radar installation operated by the U. S. Air Force and located on the Pacific coast of Washington at Neah Bay (Fig. 1). This radar provided coverage of rainfall patterns over the Pacific Ocean out to a distance of about 200 km from Neah Bay. The plan-position indicator (PPI) displays for the Neah Bay radar were recorded by time-lapse photography.

The second type of study, referred to as the Washington studies, was concerned with rainfall patterns over inland western Washington. Primary data for these studies were obtained from a network of raingages operated by the National Weather Service and by the University of Washington (UW) (Fig. 1). The time resolution of the gages operated by the Weather Service was 5–10 min in moderate rain while those operated by UW had a time resolution of 15 s in moderate rain. For the Washington studies two weather radars were operated in Seattle, one by UW (wavelength 3.2 cm, peak power 250 kW, beam width 1°) and the other (the CP-3) by the National Center for Atmospheric Research (wavelength 5.45 cm, peak power 338 kW, beam width 1°).

The PPI displays for the UW radar were recorded by time-lapse photography as the displays were cycled through a series of five gain settings. In this way, intense echo cores (shown on low-gain displays) as well as widespread light rain areas (shown on high-gain displays) could be followed in postanalysis. The CP-3 radar has a real-time color display (Gray *et al.*, 1975)

which was photographed on color motion picture film. In addition, all of the CP-3 data were recorded on magnetic tape.

3. Classification of rainbands

Rainbands observed in our case studies can be classified as follows:

Type 1. *Warm frontal.* Bands approximately 50 km in width oriented parallel to warm front and found toward the leading edge of a frontal cloud shield.

Type 2. *Warm sector.* Bands typically 50 km in width, found south of the intersection of the surface warm and cold fronts and tending to be parallel to cold fronts.

Type 3. *Cold frontal—wide.* Bands approximately 50 km in width oriented parallel to cold front and found toward the trailing edge of a frontal cloud shield.

Type 4. *Cold front—narrow.* Extremely narrow band (~5 km in width) coinciding with surface cold front.

Type 5. *Wave.* Bands occurring in a very regular pattern similar to waves, typically 10–20 km wide.

Type 6. *Post frontal.* Rainbands located in the convective cloud field behind a frontal cloud shield.

In Sections 4–6 we present examples of these six types of bands in case studies and give statistics for all of the rainbands which we have observed. In Section 7 we show that bands described by previous investigators also fall into our six categories.

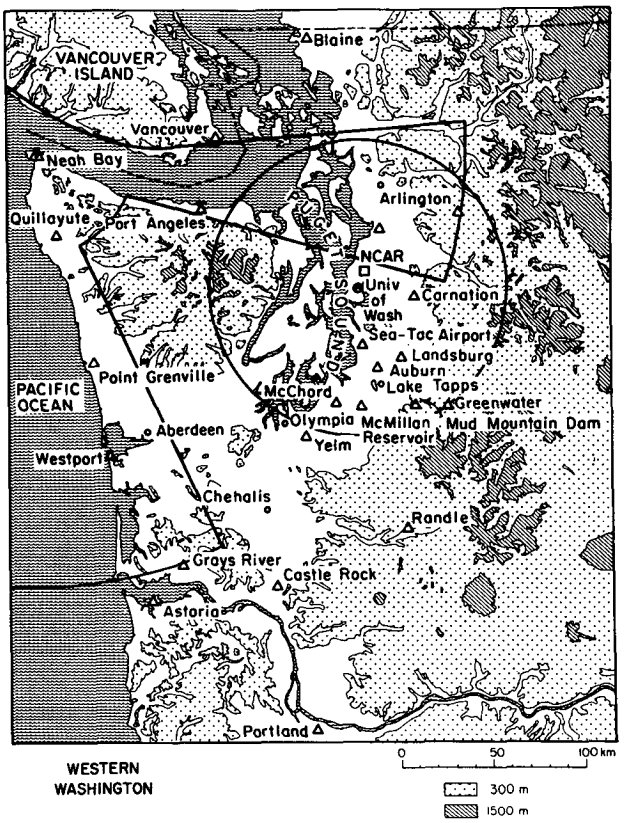

FIG. 1. Locations of field stations and types of data collected at each. Symbols indicate types of data as follows: circle, high-resolution raingage; triangle, low-resolution raingage; dot, Neah Bay radar; ×, University of Washington radars and rawinsonde; square, NCAR radar. Areas covered by the University of Washington and Neah Bay radars are enclosed by dark solid lines.

4. Example of a Pacific Ocean study

Examples of data obtained from the Neah Bay radar on 27–28 November 1973 are shown in Fig. 2. The relationship of the features observed on the radar to the large-scale storm system can be inferred from the superimposed sea-level frontal positions. When a pattern of widespread rain was located over Neah Bay, the PPI display typically appeared as shown in Fig. 2a, with a very bright echo surrounding the center of the display and extending out to ranges of up to 75 km. [The Neah Bay radar PPI displays shown in Fig. 2 are not range-corrected or quantized into various intensity levels.] Structural features embedded within the general rain area, such as band A in Fig. 2a, are seen as they existed in the region outside the central echo. Band A was located approximately parallel to the warm front and is therefore classified as Type 1. The velocity of the band normal to its orientation was 24 m s^{-1}. Band B in Fig. 2b is an example of a Type 2 band since it occurred in the warm sector. It moved northeastward, parallel to its orientation. When bands A and B passed over raingages on the Washington coast 15 min average rainfall rates were 2–5 mm h^{-1}.

Features such as bands A and B in Fig. 2 are most clearly distinguished when viewed in the form of a time lapse movie. The snapshots of the radar display shown in Fig. 2 are not a completely satisfying way to depict the results of examining the movie which emphasizes the time continuity exhibited by the rainbands. Each of the features identified as rainbands in Fig. 2 were readily tracked for several hours in the radar movies.

The surface cold front on 27–28 November was accompanied by an extremely narrow band (~2 km in width) with a continuous radar echo (band C) which is an example of a Type 4 rainband. Portions of band C can be seen in Figs. 2b and 2c. The precipitation rates which occurred as this long narrow band passed over the coastal raingage stations were consistently very high with 5–10 min average values of 25–50 mm h^{-1}. Band C was about 4 km in vertical extent.

Long, thin, continuous rainbands similar to band C, coinciding with surface cold fronts, have been observed previously by Kessler and Wexler (1960) and Browning and Pardoe (1973). The radar echo lines observed by these investigators were each followed by a 100 km wide zone of lighter precipitation. Browning and Pardoe hypothesized that the narrow rainband was an intense

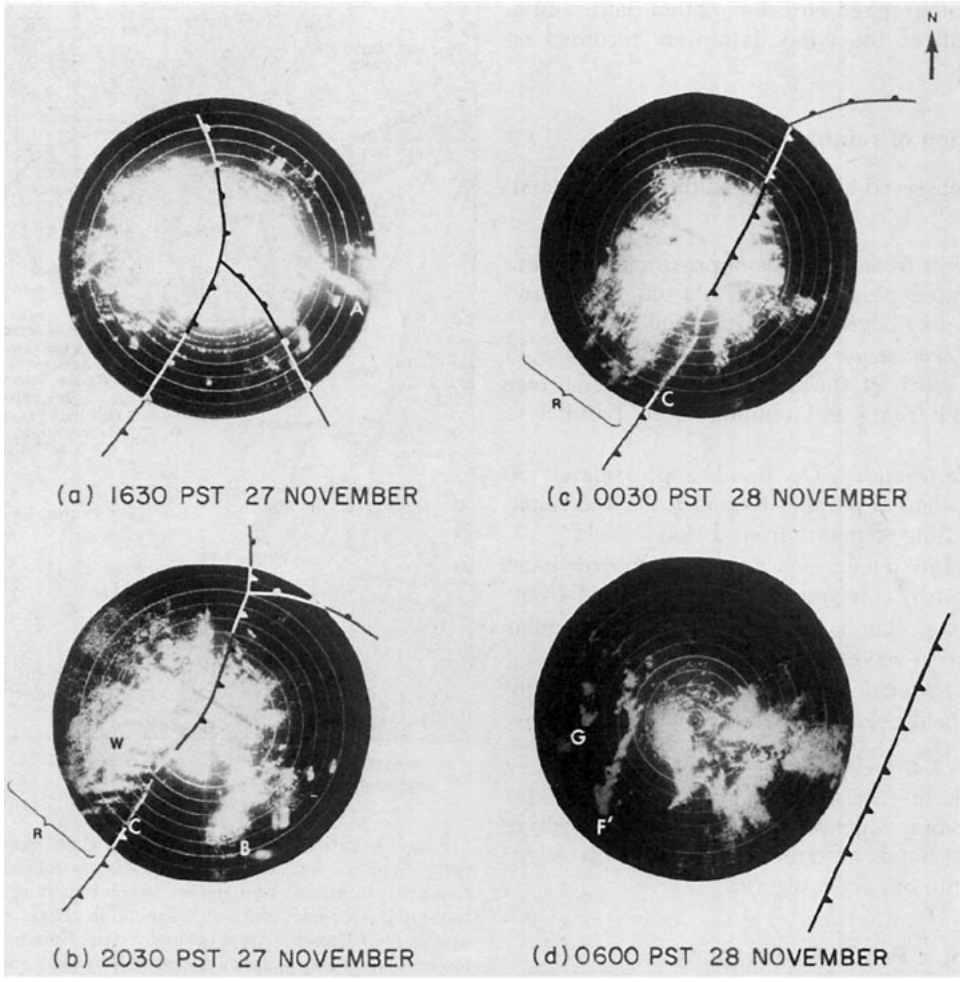

FIG. 2. Photographs of PPI displays from Neah Bay radar and sea-level frontal positions. Letters designate rainbands referred to in text. Range markers are separated by intervals of 18.5 km.

line of convection generated by lifting at the leading edge of the surface frontal zone, while the zone of lighter precipitation which followed it was due to gradual, slant-wise ascent above the sloping frontal surface. In our case, a 100 km wide zone of relatively light rain (Region R in Figs. 2b and 2c) followed the intense narrow band C, as in the cases of Kessler and Wexler and of Browning and Pardoe. However, unlike the broad bands of precipitation behind their fronts, which evidently had a fairly uniform texture, the region R in our study exhibited considerable substructure, as seen for example in Fig. 2b, where a series of wave-like bands (south and east of point W) were superimposed on R. These ripples, classified as Type 5 (wave) bands, were 15 km×70 km in average dimension and moved with the low- to mid-tropospheric winds toward the northeast parallel to the front at a speed of 32 m s^{-1}. Occasionally these waves crossed over the narrow frontal band C and as the storm passed over the Neah Bay radar, a change in orientation of the wave-like bands W was noted (Fig. 3). The periodic nature of the wave-like bands suggests that they were due to gravity waves; however, there appears to be no theory dealing with gravity waves in clouds near a sloping frontal surface with which we can compare our results.

The structure of region R varied considerably from one place to another. In addition to the wave-like bands (W in Figs. 2 and 3), region R contained portions (such as D in Fig. 3) which were characterized by patterns of irregularly-shaped small mesoscale areas. At one location (E in Fig. 3), region R contained a Type 3 (cold frontal—wide) rainband which was approximately 50 km wide and more than 100 km in length, while in other locations, such as that shown in Fig. 2c, R appeared as a broad and relatively uniform zone of weak radar echo, without any notable substructure.

After the cold front and the accompanying rainband C and region R had passed over the Washington coast, several post-frontal rainbands (Type 6) were observed on the Neah Bay radar. Post-frontal band F′ (which formed from a part of a previous band F) and post-frontal band G are shown in Fig. 2d. These bands

were typically comprised of small-scale elements, ranging in size from 10 to 1500 km² in area. The discrete structure of the post-frontal bands suggests that they were convective in nature, as would be expected since they were located in the unstable air mass behind the frontal zone.

The formation of band F′ from F is shown in Fig. 4. As the northern segment of F dissipated, F′ formed about 20 km to the east. Since the dissipation of F and the formation of F′ seem coupled, it is hypothesized that F′ was formed by the downdraft from the rainband F as it dissipated. The development of new convective elements from the downdrafts spreading out from old clouds and providing lift for the surrounding unstable air is a commonly observed feature of cumulonimbus clouds (Byers and Braham, 1949; Newton, 1963; Zipser, 1969). The curved shape of F′, first apparent at 0440 PST in Fig. 4, would be expected if the new band was forming at the edge of divergent, cold downdraft air spreading out from a dissipating element of F.

5. Example of a Washington study

In the Washington studies, precipitation patterns were deduced from raingage data using a procedure

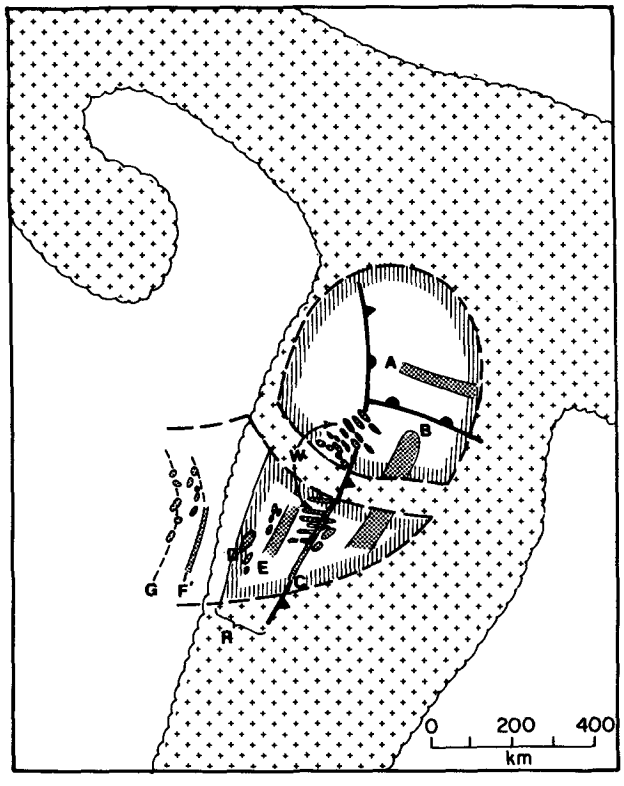

FIG. 3. Schematic representation of storm observed on 27–28 November 1973. Scalloped boundary encloses cloud pattern observed by satellite. Dashed lines enclose portion of cloud shield which passed over area of radar observations. Hatching encloses light rain areas; heavy rain areas are indicated by stippling. Letters refer to features mentioned in text. Sea-level fronts are shown.

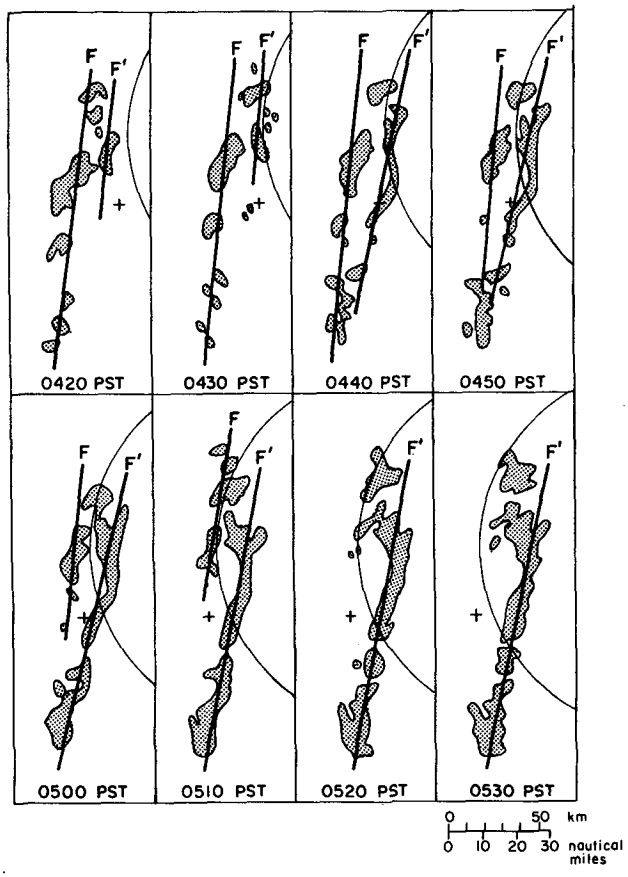

FIG. 4. Formation of rainband F′ from F as seen on the Neah Bay radar. Cross is at 47°N and 127°W, and circle segment is 100 km from the radar site.

similar to that of Elliott and Hovind (1964). Plots of 15 min average rainfall rates were arranged in order of their geographical situation, and similarities in the time distributions of the rainfall rates were noted and labeled, as shown in Fig. 5. The features denoted B_1–B_4 in Fig. 5 were four rainbands embedded in an occluded frontal cloud system which passed over western Washington on 20 December 1973. Based on mapped isochrones of the front and back edges of each rainband, their positions at any given time could be determined, as shown in Fig. 6.

In comparing raingage traces such as in Fig. 5, there is some subjectivity in deciding on the boundaries of features such as B_1–B_4. The chosen boundaries were checked in two ways. First it was assumed that the large bands moved in a more or less continuous manner over the raingages. Hence, the boundaries were required to conform to reasonably continuous isochrone patterns for both front and back edges. Second, whenever the bands were within the area of coverage of the UW weather surveillance radar, the band structure deduced from the raingage data had to be *consistent* with the radar data (see Fig. 6). The radar echoes seen within the rainbands in Fig. 6 do not look like bands them-

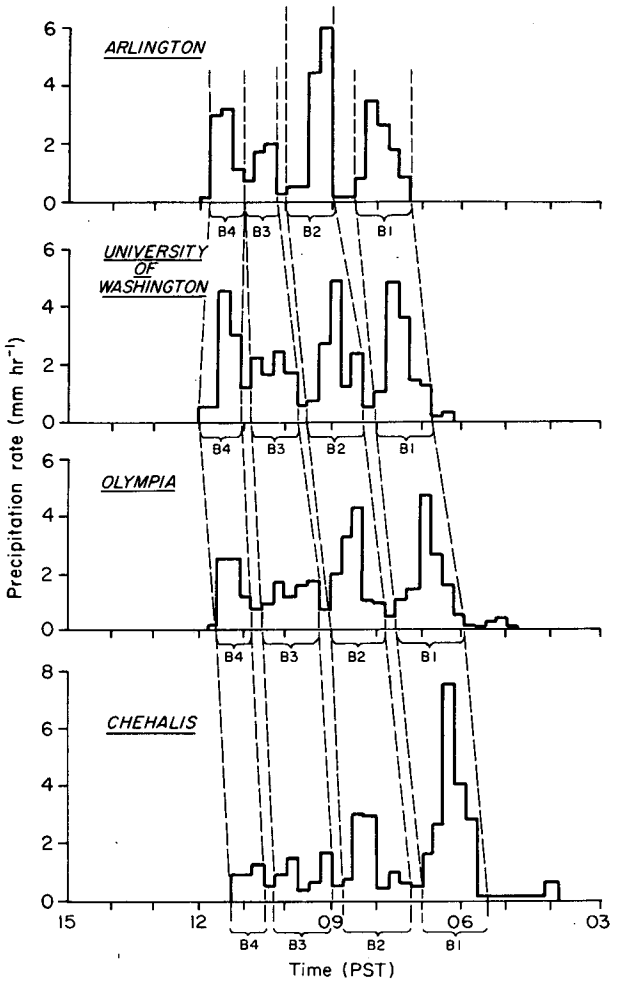

FIG. 5. Precipitation rate at stations along an approximately north-south line on 20 December 1973. Lines connecting plots show front and back edges of rainbands B_1–B_4.

selves because the UW radar range limitation (circle in Fig. 1) precludes the entire rainband from appearing on the radar scope. However, the echoes which did appear were expected to fall within and move in a manner consistent with the rainbands deduced from raingage data. If they did not, the raingage isochrone analysis was revised accordingly. Revisions were generally minor, and the final analyses did not violate any observations. Often the radar data were particularly helpful in locating the leading edges of rainbands. A final check of the time continuity and progression of the rainbands over Washington was made by constructing a time-lapse movie from a series of maps showing the instantaneous positions of rainbands B_1–B_4.

Properties of bands B_1–B_4 are summarized in Table 1. Generally, all of the bands were very similar, except in their orientation. The first two bands (B_1 and B_2) were oriented along a northwest to southeast line, while B_3 and B_4 were oriented nearly north-south. Detailed synoptic analysis, based in part on serial rawinsondes launched from UW at intervals of 2–3 h (Houze, *et al.*, 1976), showed that the earlier bands B_1 and B_2 occurred with the passage of the warm front (of an occlusion) aloft, while the two later bands were associated with the passage of a double cold front aloft. Hence, B_1 and B_2 are examples of Type 1 (warm frontal) rainbands, while B_3 and B_4 are examples of Type 3 (cold frontal—wide) rainbands. The relationship of the rainbands B_1–B_4 to the fronts on 20 December is indicated schematically in Fig. 7.

It is evident from the superimposed radar echoes in Fig. 6 that a pattern of small-scale areas of high-intensity rainfall existed within each of the large bands. The small-scale elements embedded in rainbands B_1–B_4 were investigated by identifying and tracking the horizontal motion of individual radar echoes appearing in

TABLE 1. Characteristics of rainbands observed on 20 December 1973. Numbers in parentheses are extreme values.

Rainband	Period of observation (PST)	Number of stations passed over	Mean rainfall rate (mm h^{-1})	Maximum rainfall rate (mm h^{-1})	Mean duration over a station (min)	Mean amount of rain at a station (mm)	Width (km)	Orientation*	Velocity normal to band orientation (m s^{-1})
B_1	0445–1000	17	2.8 (1.8–5.1)	12.4 for 1 min	69 (45–105)	3.3 (1.8–7.6)	75 (24–117)	NW–SE to NNW–SSE	18 from SW to NE
B_2	0715–1100	16	2.6 (0.8–4.1)	13.8 for 1 min	66 (30–105)	2.7 (0.8–6.1)	74 (19–145)	NW–SE	20 from SW to NE
B_3	0700–1245	13	2.2 (1.0–6.4)	21.3 for 5 min	56 (30–90)	2.1 (0.4–7.1)	48 (29–68)	N–S to NNW–SSE	16 from W to E
B_4	0830–1230	17	2.6 (0.5–6.8)	15.2 for 7 min	55 (30–90)	2.5 (0.4–10.2)	50 (15–72)	N–S	14 from W to E

* Relative to true north.

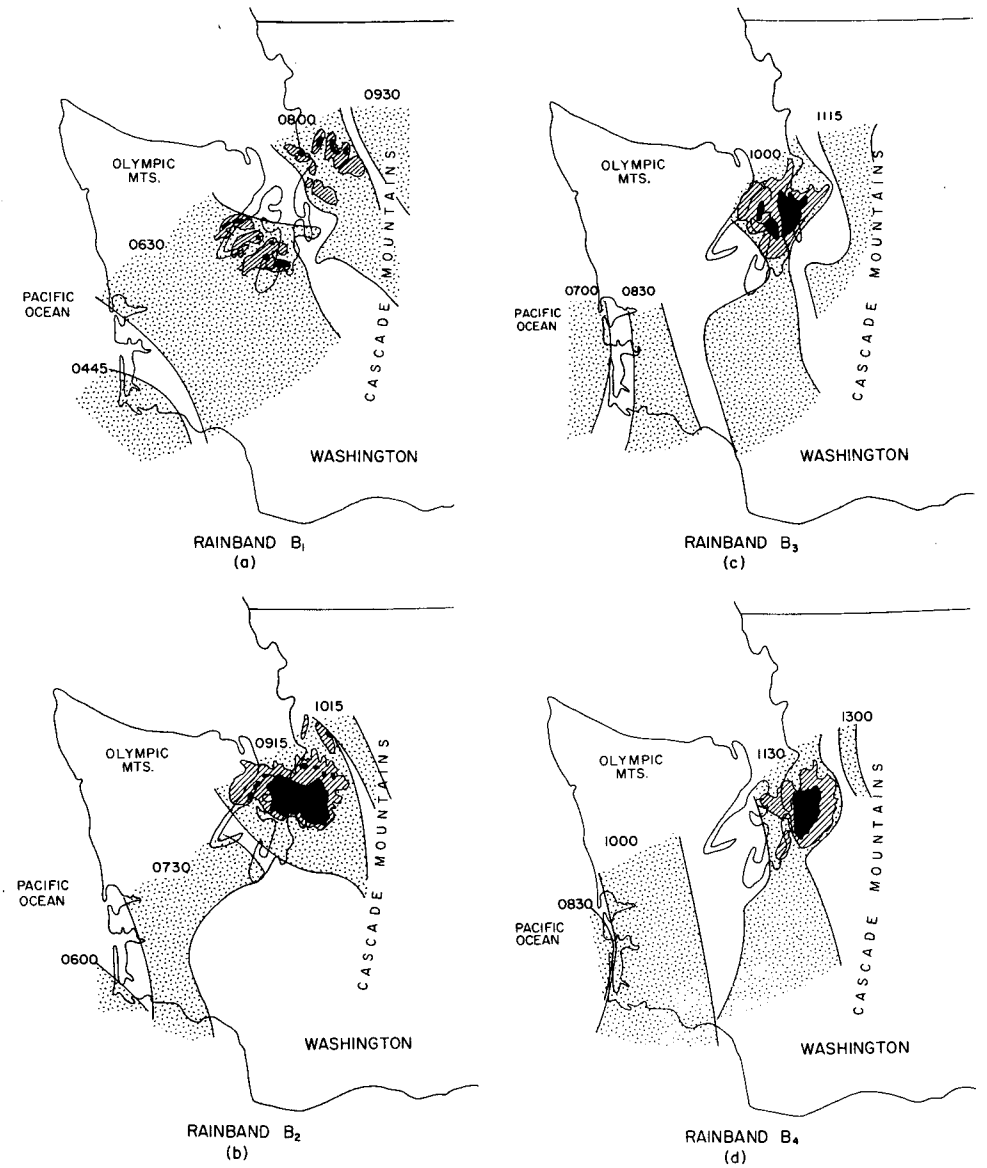

FIG. 6. Rainbands B_1–B_4 at different times (PST) during their passage over western Washington. Stippling indicates rainband positions deduced from raingage data. Hatching shows maximum gain echoes seen on University of Washington radar. Black areas are minimum gain echoes.

the PPI displays of the UW radar. To minimize the effects of varying range on the sampled echoes, two reference areas (shown in Fig. 8) were chosen for echo sampling. These areas were picked because they were relatively free of ground clutter and confined to a small range interval between 30 and 60 km from the radar site.

The average areas, concentrations and motions of the echoes sampled at two receiver gain settings (maximum H and minimum L) are listed in Table 2. The sampled echoes (described in Table 2) ranged from 10 to 500 km^2 in area. Previous investigators (e.g., Browning and Harrold, 1969; Austin and Houze, 1972) have also found that small-scale elements of this size were embedded in large mesoscale rain areas such as B_1–B_4. The small-scale echo motions indicated in Table 2 are in close agreement with the winds between 850 and 700 mb with the best agreement at 700 mb. Detailed analysis of rawinsonde, aircraft and Doppler radar data (Houze *et al.*, 1976) shows that this was the layer in which most of the precipitation in the small-scale areas was generated.

6. Rainbands in other occluded cyclones

We have examined the precipitation in nine other occluded cyclones, in addition to those described in

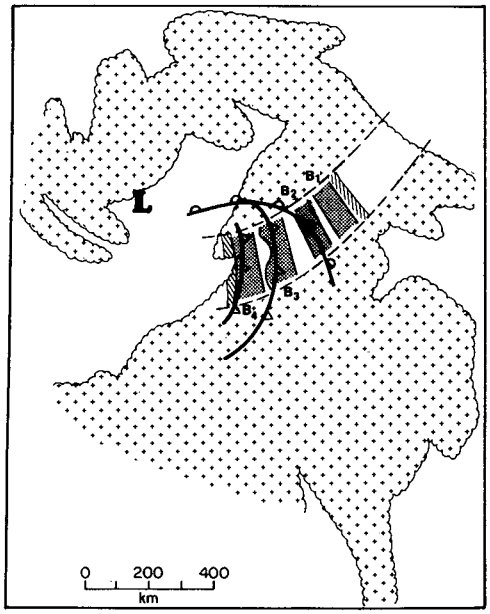

FIG. 7. Schematic representation of rainbands B_1–B_4 at an instant of time in the storm of 20 December 1973. Scalloped contour outlines cloud pattern observed by satellite. Dashed lines enclose portion of cloud shield which passed over area of observations. Hatching encloses light rain areas; heavy rain areas are indicated by stippling. Letters refer to features mentioned in text. Fronts shown are for 720 mb level.

Sections 4 and 5, and have noted that rainbands occurred in each of these occlusions. All but one rainband could be identified as one of the six types listed in Section 3, and each type of rainband was observed in more than one occlusion. Table 3 summarizes the characteristics of all of the rainbands that we have examined.

In Table 3, small areas within the rainbands are indicated as "not observed" for band Types 1–5 in the Pacific studies. Since the Neah Bay radar display was not systematically quantized into a series of echo intensity levels, it was not possible to detect small echo cores embedded within the bands, except in Type 6 (post-frontal) bands which were composed of lines of very discrete small-scale echoes. From the Washington studies listed In Table 3, in which observations were made with the quantized UW radar, it is evident that small mesoscale areas were, in fact, located within rainbands of Types 1, 2, 3 and 5.

Although our results indicate a tendency for rainbands to occur in occluded cyclones, and for the bands to be of six types, it should be noted that the rainbands which we observed did not always occur in the same sequence or combination. In some cases rainbands were interspersed with large, irregularly shaped regions of light rain (100's of km in dimension), while in other cases small non-banded mesoscale rain areas (10's of km in dimension) occurred between the bands. Fig. 9 illustrates the various arrangements of rainbands in several of our case studies.

The two rainbands shown in Fig. 9a were classified as Type 1 (warm frontal) since they were located toward the leading edge of the frontal cloud shield and were parallel to the surface warm front. A frontal wave formed on the cold front of the occlusion shown in Fig. 9a and on the next day the new wave appeared as it is shown in Fig. 9b. The two rainbands observed in Fig. 9b were designated as Type 2 (warm sector bands) because of their position in the warm sector of the wave. As the cold front associated with the wave moved through western Washington, it was preceded by a Type 3 (warm-sector) band and accompanied by a Type 2 (wide cold-frontal) band (Fig. 9c).

The six large rainbands shown in Figs. 9a–c were interspersed with numerous small non-banded mesoscale areas. This is illustrated by the raingage record shown in Fig. 10. The peaks labeled C_1–C_7 were determined (by observations made with the UW radar) to be associated with small non-banded mesoscale rain areas (~50 km in dimension) moving over the raingage site. In this storm, the small mesoscale areas outside of the large rainbands contributed almost as much to the total rainfall as did the bands themselves. A more detailed description of the rainfall patterns on 5–7 December 1973 (cases shown in Figs. 9a–c and Fig. 10) may be found in Shieh (1975).

Figs. 9d and 9e show examples of occluded frontal systems which each contained a single Type 3 (wide

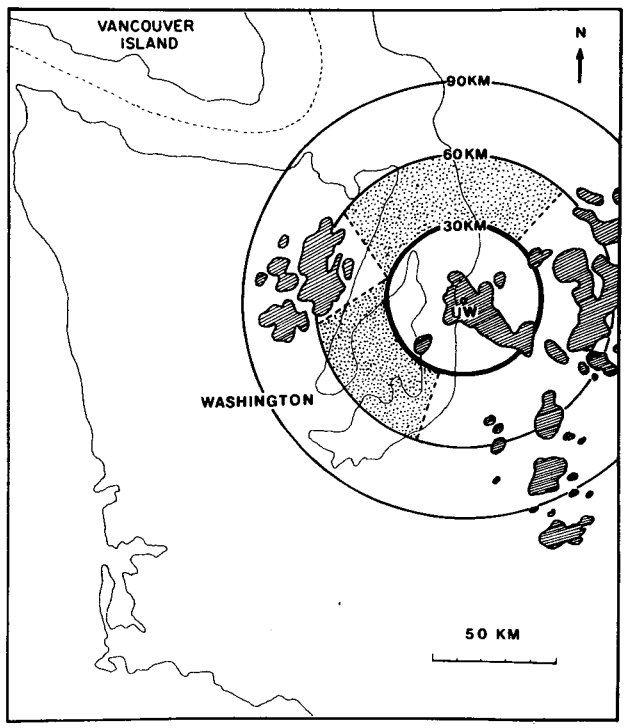

FIG. 8. Reference areas for radar echo sampling (stippled areas between 30 and 60 km). Circles are at indicated distances from radar at University of Washington (UW). Ground echoes are indicated by hatching.

TABLE 2. Characteristics of the small-scale elements embedded in the rainbands observed on 20 December 1973. H and L refer to high- and low-gain echoes, respectively.

Rainband	Concentration of echoes (number per 10^3 km^2) H	L	Echo size (km^2) H	L	Echo velocity (deg/m s^{-1}) H	L	Winds aloft (deg/m s^{-1}) 850 mb	700 mb	500 mb
B_1	1.1	1.9	431	30	220/26	220/24	160/18	220/28	215/40
B_2	1.4	0.8	523	85	225/28	230/32	180/22	210/35	210/40
B_3	0.9	0.6	112	12	220/33	215/33	200/30	220/38	210/40
B_4	1.7	0.6	43	36	230/29	225/26	200/30	210/32	210/42

cold-frontal) band. Examples of rainbands accompanied by large regions of non-banded light precipitation are seen in Figs. 9d and 9f. In the case of 7 January 1975 (Fig. 9f), the first large non-banded region had a very uniform structure, while the second contained a pattern of smaller mesoscale and cumulus-scale elements, including some small Type 5 wave-like bands. These Type 5 bands are shown in Fig. 11 as they appeared on radar. Each of these small bands (tracked in time-lapse movies of the radar PPI) moved over the area of radar coverage shown in Fig. 11 and exhibited a definite band-like character while it was in the middle of the area (e.g., band W_2 in Fig. 11).

7. Rainbands in other geographical areas

The above results suggest that the six types of bands occur rather generally in extratropical cyclones. This conclusion is further supported by the fact that rainbands observed in extratropical cyclones in other parts of the world fit nicely into our classification. Rainbands parallel to and ahead of warm fronts have been observed in open wave cyclones by Browning and Harrold (1969) and Reed (1972). These bands would be Type 1 in our classification. Browning and Harrold's observations were over the British Isles, while Reed's were in New England. Similar rainbands, with warm frontal orientation, were found in the leading (eastern) portions of occluded frontal systems described by Nagle and Serebreny (1962) over the eastern Pacific Ocean and by Kreitzberg and Brown (1970) over the northeastern United States.

In the frontal systems studied by Nagle and Serebreny (1962) and Kreitzberg and Brown (1970), the Type 1 bands in the leading portion of the cloud shield gave way to bands with cold frontal orientations (which would be Type 2 by our classification) in the trailing western portion. In an occluded cyclone over the northeastern Atlantic Ocean, Browning *et al.* (1973) observed a series of Type 2 bands parallel to multiple cold fronts aloft. Their Type 2 bands, however, were apparently not preceded by a series of warm frontal bands.

Warm sector bands (Type 3) were observed frequently in open wave cyclones near Japan by Nozumi and Arakawa (1968). They found that the warm sector

TABLE 3. Average characteristics of rainbands observed in eleven occluded frontal systems. Dash indicates not observed. H and L refer respectively to high- and low-gain radar echoes which were analyzed separately for the Washington cases.

Type of band	Number of cases	Width (km)	Rain rate (mm h^{-1})	15-min peak rain rate (mm h^{-1})	Size of small areas (km^2)		Number of small areas per 10^3 km^2		Absolute value of difference between velocity of small area and winds at pressure level indicated (deg/m s^{-1})					
									850 mb		700 mb		500 mb	
Pacific studies														
1. Warm frontal	1	15	7	7	—		—		—		—		—	
2. Warm sector	1	40	3	7	—		—		—		—		—	
3. Cold frontal wide	4	44	—	—	—		—		—		—		—	
4. Cold frontal narrow	2	6	28	*	—		—		—		—		—	
5. Wave	1	15	—	—	—		—		—		—		—	
6. Post frontal	15	20	4	5	270		2.9		15°/4		14°/5		12°/21	
Washington studies					H	L	H	L	H	L	H	L	H	L
1. Warm frontal	4	60	3	7	400	60	1.8	1.8	29°/4	33°/8	9°/7	7°/3	13°/13	11°/10
2. Warm sector	3	50	2	7	210	35	2.0	0.8	13°/3	10°/5	8°/4	8°/5	13°/6	17°/1
3. Cold frontal wide	8	65	3	11	200	40	2.3	1.4	28°/7	24°/6	11°/6	11°/4	18°/10	13°/5
4. Cold frontal narrow	0	—	—	—	—	—	—	—	—	—	—	—	—	—16
5. Wave	1	21	1	5	—	—	—	—	—	—	—	—	—	—
6. Post frontal	2	51	2	9	90	55	1.4	0.7	14°/4	17°/4	13°/1	13°/1	5°/1	10°/

* Duration over station less than 15 min.

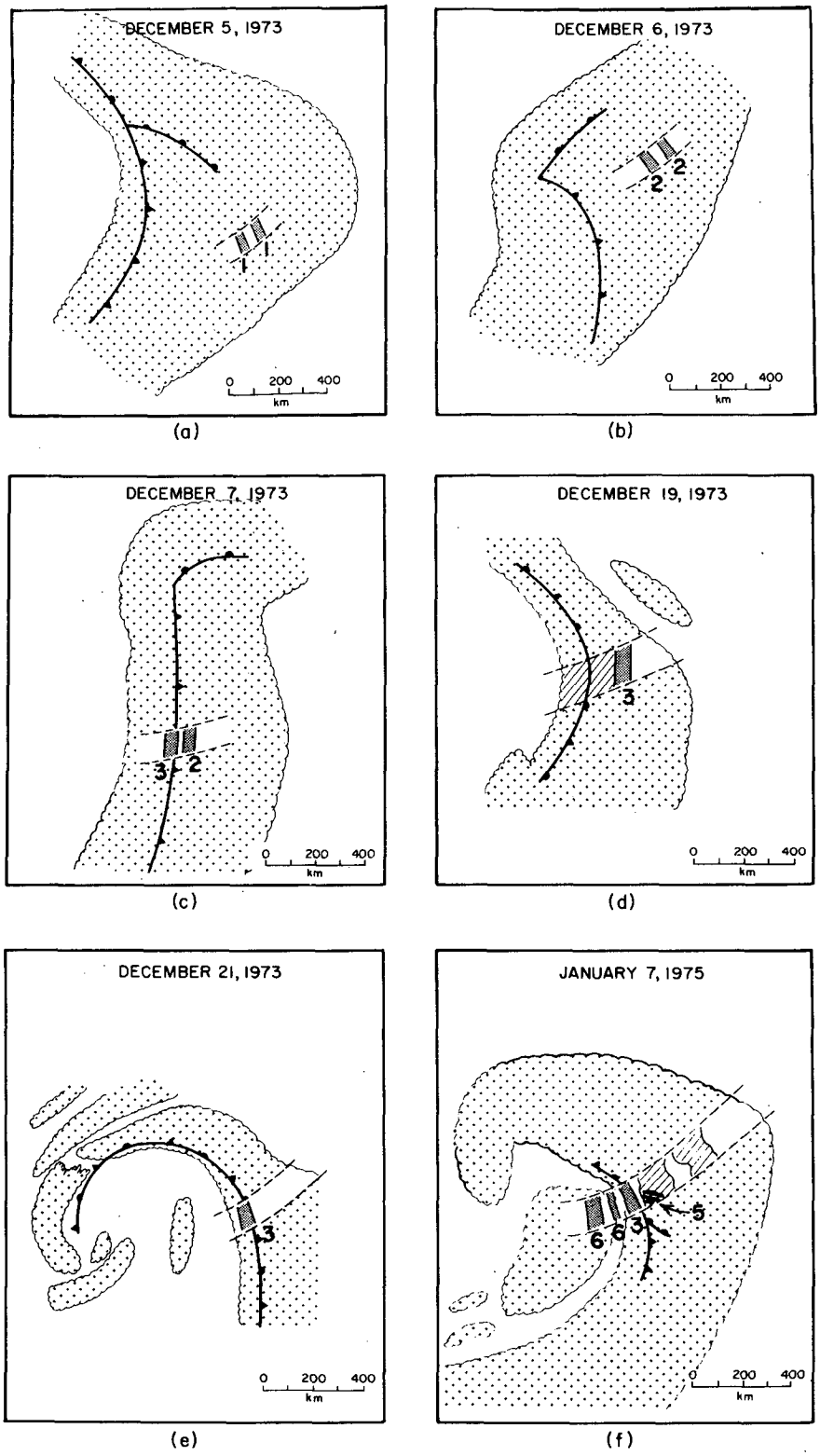

FIG. 9. Schematic representation of rainbands observed in six frontal cloud systems. Scalloped borders outline cloud pattern shown in satellite data. Numbers refer to band types discussed in text. Hatching indicates areas of light non-banded rain. Surface frontal positions are shown. Dashed lines enclose portions of cloud shields which were observed.

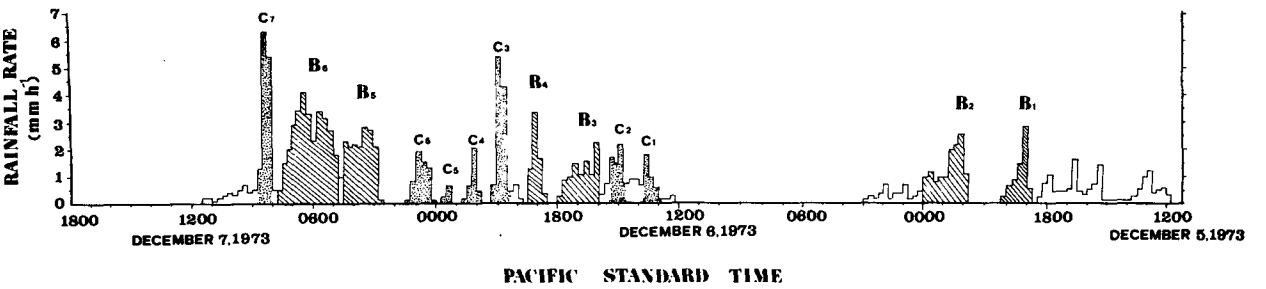

FIG. 10. Rainfall rate at University of Washington site in Seattle, 5–7 December 1973.

bands tended to be parallel to the cold front, often intersecting the warm front at right angles. Harrold (1973) also reported that warm sector bands parallel to the cold front occurred frequently in cyclones near the British Isles. Browning and Harrold (1969) found warm-sector rainbands over England which were not parallel to either the cold or warm front in a wave depression; however, the orientation of these bands may have been influenced by the topography of the British Isles. The prefrontal squall line associated with severe convective storms is a notable special case of Type 3 (warm sector) rainband.

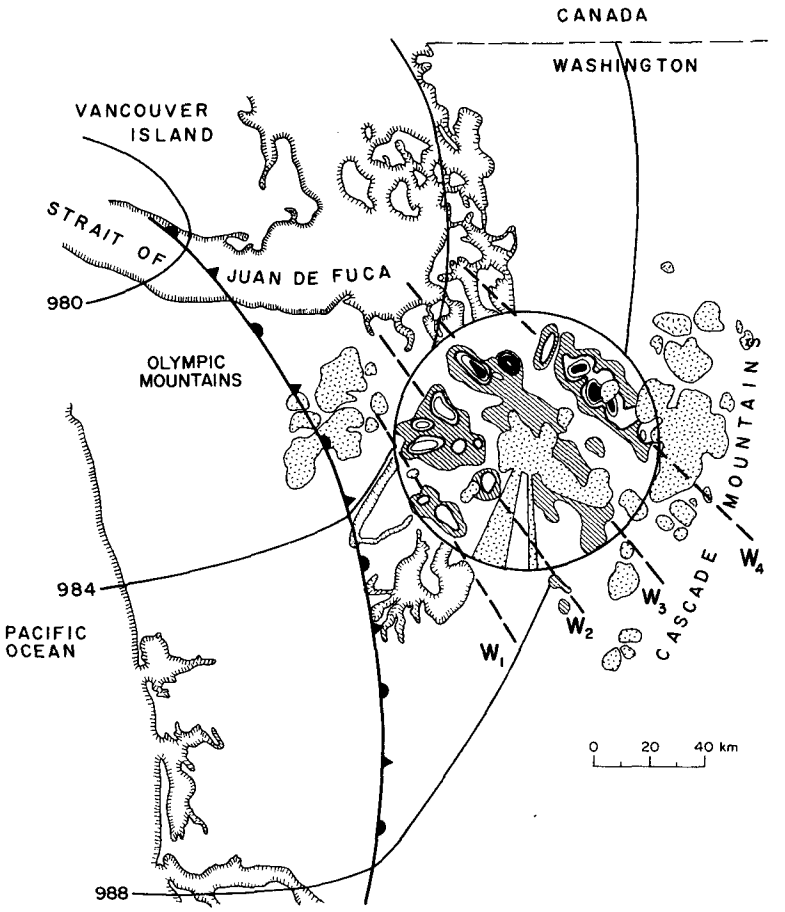

FIG. 11. Four wave-like rainbands (W_1–W_4) observed on University of Washington radar at 1715 PST 7 January 1975. Dashed lines show the axes of the bands which were moving from southwest to northeast across the area of radar coverage. Quantized precipitation echo contours in the rainbands are shown for five intensity levels. Hatching shows weakest portions of echoes. White inside of solid black shows strongest precipitation cores. Ground echoes and blocked sectors are shown by stippling. Only exceptionally intense precipitation signals were detected outside the circle (radius 50 km) centered on the radar site.

As noted in Section 3, Type 4 rainbands have been observed previously by Kessler and Wexler (1960) in New England and by Browning and Pardoe (1973) in six cases over the British Isles.

Postfrontal convective rainbands (Type 6) were included by Nagle and Serebreny (1962) in their schematic model of radar echoes in occluded cyclones over the eastern Pacific Ocean. The occurrence of mesoscale precipitation bands in cold air masses to the west of surface cyclonic systems is a well known phenomenon during the winter over the Sea of Japan (e.g., Matsumoto *et al.*, 1967).

8. Conclusions

We have examined the rainfall patterns in eleven occluded cyclones in the Pacific Northwest. When presented against the background of previous work on mesoscale precipitation patterns, our results provide a more complete summary of rainbands in extratropical cyclones than has been available previously. Six types of rainbands have been identified and each type has been observed repeatedly in cyclonic rainstorms in the Pacific Northwest. Rainbands observed in mid-latitude cyclones in other parts of the world all appear to fit into our six categories. One type of band, the very regular small wave-like band (Type 5), has only been reported in our case studies. Except for the Type 5 bands, all of the rainbands show a strong tendency to be parallel to either the warm front or the cold front of the parent cyclonic storm.

The large rainbands in our study contained small mesoscale elements (10–500 km^2 in area) of maximum rainfall intensity. These small mesoscale areas, in concentrations of 1–3 per 1000 km^2, were most pronounced in the post-frontal (Type 6) bands. The small mesoscale areas within the rainbands moved with the wind between 850 and 700 mb.

The fact that the precipitation in extratropical cyclones is concentrated in rainbands, and within still smaller mesoscale elements within the rainbands, indicates that the problem of understanding frontal precipitation processes is largely one of understanding the dynamics and cloud microphysics of the individual mesoscale areas. In future work, progress can be expected if the identification of mesoscale areas by raingage and conventional radar observations is combined with detailed aircraft and Doppler radar measurements of the dynamical and microphysical properties of the mesoscale systems. Studies of this type are now underway as part of the CYCLES Project at the University of Washington.

Acknowledgments. This research was supported by Grants GA-40806 and DES-7414726 from the Atmospheric Sciences Section of the National Science Foundation and by Contract F19628-74-C-0066 from Air Force Cambridge Research Laboratories.

We wish to thank all members of the University of Washington's Cloud Physics Group who helped in this study. Thanks are also due to the Commanding Officer of the Makah Air Force Station for allowing us access to the Neah Bay radar data, and to the Field Observing Facility of the National Center for Atmospheric Research (which is sponsored by the National Science Foundation) for operating the CP-3 radar and for the loan of a rawinsonde unit.

REFERENCES

Austin, P. M., and R. A. Houze, Jr., 1972: Analysis of the structure of precipitation patterns in New England. *J. Appl. Meteor.*, **11**, 926–935.

Browning, K. A., 1974: Mesoscale structure of rain systems in the British Isles. *J. Meteor. Soc. Japan*, **50**, 314–327.

——, and T. W. Harrold, 1969: Air motion and precipitation growth in a wave depression. *Quart. J. Roy. Meteor. Soc.*, **95**, 288–309.

——, and C. W. Pardoe, 1973: Structure of low-level jet streams ahead of mid-latitude cold fronts. *Quart. J. Roy. Meteor. Soc.*, **99**, 619–638.

——, M. E. Hardman, T. W. Harrold and C. W. Pardoe, 1973: The structure of rainbands within a mid-latitude depression. *Quart. J. Roy. Meteor. Soc.*, **99**, 215–231.

Byers, H. R., and R. R. Braham, Jr., 1949: *The Thunderstorm.* Washington, D.C., U. S. Weather Bureau, 287 pp. (see pp. 77–79).

Elliott, R. D., and E. L. Hovind, 1964: On convection bands within Pacific coast storms and their relation to storm structure. *J. Appl. Meteor.*, **3**, 143–154.

Gray, G. R., R. J. Serafin, R. E. Rinehart and J. J. Boyajean, 1975: Real-time color Doppler radar display. *Bull. Amer. Meteor. Soc.*, **56**, 580–588.

Harrold, T. W., 1973: Mechanisms influencing the distribution of precipitation within baroclinic disturbances. *Quart. J. Roy. Meteor. Soc.*, **99**, 232–251.

——, and P. M. Austin, 1974: The structure of precipitation systems—a review. *J. Rech. Atmos.*, **8**, 41–57.

Hobbs, P. V., R. A. Houze, Jr., and T. J. Matejka, 1975: The dynamical and microphysical structure of an occluded frontal system and its modification by orography. *J. Atmos. Sci.*, **32**, 1542–1562.

Houze, R. A., J. D. Locatelli and P. V. Hobbs, 1976: Dynamics and microphysics of rainbands in an occluded frontal system. *J. Atmos. Sci.* (submitted for publication).

Kessler, E., and R. Wexler, 1960: Observations of a cold front, 1 October 1958. *Bull. Amer. Meteor. Soc.*, **41**, 253–257.

Kreitzberg, C. W., and H. A. Brown, 1970: Mesoscale weather systems within an occlusion. *J. Appl. Meteor.*, **9**, 417–432.

Matsumoto, S., K. Ninomiya and T. Akiyama, 1967: A synoptic and dynamic study on the three-dimensional structure of mesoscale disturbances observed in the vicinity of a cold vortex center. *J. Meteor. Soc. Japan*, **45**, 64–81.

Nagle, R. E., and S. M. Serebreny, 1962: Radar precipitation echo and satellite observations of a maritime cyclone. *J. Appl. Meteor.*, **1**, 279–295.

Newton, C. W., 1963: Dynamics of severe convective storms. *Meteor. Monogr.*, No. 27, 33–58.

Nozumi, Y., and H. Arakawa, 1968: Prefrontal rainbands located in the warm sector of subtropical cyclones over the ocean. *J. Geophys. Res.*, **73**, 487–492.

Reed, R. W., 1972: Characteristics and development of mesoscale precipitation areas in extra-tropical cyclones. S.M. thesis, Massachusetts Institute of Technology, 94 pp.

Shieh, S.-L., 1975: Mesoscale precipitation patterns in an occluded frontal system. M.S. thesis, University of Washington, 73 pp.

Zipser, E. J., 1969: The role of organized unsaturated convective downdrafts in the structure and rapid decay of an equatorial disturbance. *J. Appl. Meteor.*, **8**, 799–814.